Atmos. Meas. Tech., 10, 667–680, 2017
www.atmos-meas-tech.net/10/667/2017/
doi:10.5194/amt-10-667-2017

Atmospheric Measurement Techniques
Open Access

Six years of atmospheric CO_2 observations at Mt. Fuji recorded with a battery-powered measurement system

Shohei Nomura[1], Hitoshi Mukai[1], Yukio Terao[1], Toshinobu Machida[1], and Yukihiro Nojiri[1,2]

[1]Center for Global Environmental Research, National Institute for Environmental Studies, 16-2 Onogawa, Tsukuba, Ibaraki, 305-8506, Japan
[2]Department of Earth and Environmental Sciences, Hirosaki University, Bunkyo-1, Hirosaki, Aomori, 036-8560, Japan

Correspondence to: Shohei Nomura (nomura.shohei@nies.go.jp)

Received: 1 September 2016 – Discussion started: 6 October 2016
Revised: 30 January 2017 – Accepted: 12 February 2017 – Published: 3 March 2017

Abstract. We developed a battery-powered carbon dioxide (CO_2) measurement system for monitoring at the summit of Mt. Fuji (3776 m a.s.l.), which experiences very low temperatures (below −20 °C) and severe environmental conditions without access to gridded electricity for 10 months (from September to June). Our measurement system used 100 batteries to run the measurement unit during these months. These batteries were charged during the 2-month summer season when gridded electricity was available, using a specially designed automatic battery-charging system. We installed this system in summer 2009 at the Mt. Fuji weather station; observations of atmospheric CO_2 concentration were taken through December 2015. Measurements were never interrupted by a lack of battery power except for two cases in which lightning damaged a control board. Thus we obtained CO_2 data during about 94 % of the 6-year period. Analytical performances (stability and accuracy) were better than 0.1 ppm, as tested by checking working standards and comparisons with flask sampling.

Observational results showed that CO_2 mole fractions at Mt. Fuji demonstrated clear seasonal variation. The trend and the variability of the CO_2 growth rate observed at Mt. Fuji were very similar to those of the Mauna Loa Observatory (MLO). Seasonally, the concentration at Mt. Fuji was 2–10 ppm lower in summer and 2–12 ppm higher in winter than those at MLO. The lower concentrations at Mt. Fuji in summer are mainly attributed to episodes of air mass transport from Siberia or China, where CO_2 is taken up by the terrestrial biosphere. On the other hand, the relatively higher concentrations in winter seem to reflect the high percentage of air masses originating from China or Southeast Asia during this period, which carry increased anthropogenic carbon dioxide. These results show that Mt. Fuji is not very influenced by local sources but rather by the sources and sinks over a very large region.

Thus we conclude that, as this system could provide stable measurement data with relatively easy operation for 6 years at Mt. Fuji, it could be a useful monitoring technique for remote background sites elsewhere.

1 Introduction

In order to quantitatively understand the global carbon cycle, long-term observations of atmospheric CO_2 concentrations have been performed at "background sites" where the observed air is less affected by local sinks and sources, such as Mauna Loa in Hawaii and Antarctica (Keeling et al., 1989, 2001; Conway et al., 1994). On the other hand, the importance of observations at "regional sites" has also been recognized when analyzing regional sinks and sources using an inverse model with data from various ground observation sites, such as Siberia and China (Maksyutov et al., 2003; Saeki et al., 2013; Zhang et al., 2014).

Globally, atmospheric CO_2 concentrations are currently observed at about 180 sites, including both background and regional sites, although their distribution is not uniform (WMO, 2015). For example, there are insufficient sites in Southeast and East Asia, regions in which economies have grown rapidly in this decade. In particular, China is now known as the country with the greatest CO_2 emissions in the world (CDIAC 00001_V2016; Boden et al., 2016), so

Published by Copernicus Publications on behalf of the European Geosciences Union.

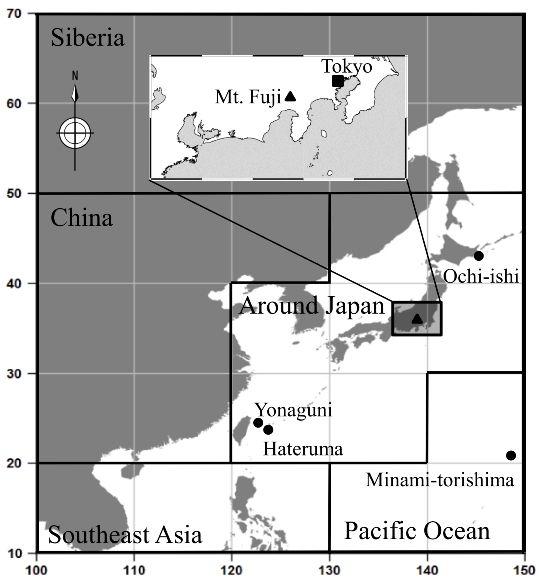

Figure 1. Location of Mt. Fuji (35.21° N, 138.43° E) and of other sites representative for the long-term observation of atmospheric CO_2 concentration in Japan (small black dots), and the five areas used for back-trajectory analysis of air mass origins (Siberia, China, Southeast Asia, around Japan, and Pacific Ocean).

more observation sites are needed. Representative sites for the long-term observation of atmospheric CO_2 concentrations in Japan are located in the higher- and lower-latitude coastal areas of Ochi-ishi, Minamitori Island, Hateruma Island, and Yonaguni Island (Fig. 1; Watanabe et al., 2000; Mukai et al., 2001).

Midlatitude regions of Japan are mostly affected by regional air mass transport via the prevailing westerlies from the Asian continent. However, suitable CO_2 observation sites are lacking because of the distribution of industrial and populated areas. Obtaining CO_2 observations in the midlatitude Asian region would be advantageous for monitoring changes in the carbon cycle, because many countries in this region are growing economically with associated increases in their CO_2 emissions.

Mt. Fuji, the highest mountain in Japan (3776 m a.s.l.), is a well-suited site for monitoring CO_2 concentrations. Its summit is located in the free troposphere, which means it is not affected directly by air at ground level for most of the year (Tsutsumi et al., 1994). Mt. Fuji is positioned in the center of Japan (Fig. 1), and the air masses that pass over it are mainly affected by the regional air characteristics of the Asian continent (Igarashi et al., 2004). Nakazawa et al. (1984) performed observations of CO_2 concentration at the summit in October 1980 and July–October 1981, with the following findings: (i) the CO_2 concentration was not influenced by wind direction; (ii) diurnal variation of CO_2 concentration was not observed; (iii) CO_2 concentrations were in close agreement with vertical profiles derived from aircraft measurements near Sendai, Japan; and (iv) CO_2 variations were caused by air masses transported from different regions such as the Pacific Ocean and the Asian continent; (v) The observed annual rate of increase was comparable with the rate derived from aircraft measurements over Japan at an equivalent altitude to the summit. Therefore, they suggested that observations obtained at the summit of Mt. Fuji could be considered representative of the free-tropospheric CO_2 concentration in the midlatitude Asian region. Sawa et al. (2005) performed continuous observations of CO_2 and CO at the summit from September 2002 to February 2003 and from May 2003 to May 2004, with the following findings: (i) many episodic events showed large enhancements of CO_2, and (ii) episodic enhancements clearly associated with increased CO peaks were observed at the same time.

After 2004, CO_2 observations at the summit of Mt. Fuji were interrupted because of the shutdown of manual operations at the Mt. Fuji weather station by the Japan Meteorological Agency (JMA). Although the JMA continued automatic meteorological observations, commercial power has only been available during 2 months in the summer since 2004. Therefore, it became difficult to maintain whole-year observations at the station without a power supply and a heating and air-conditioning system.

In this study, we developed a CO_2 measurement system that can be operated without gridded electricity, even under the harsh conditions found at the summit of Mt. Fuji, where the weather can be extremely cold in winter and other severe weather conditions such as high wind velocity and frequent lightning are encountered. It is impossible for an ordinary person to go there from September until July. Low atmospheric pressure (about 650 hPa) makes manual maintenance work difficult and also causes reduced sensitivity in infrared (IR) absorption detection in the system. Our system was insulated to protect it against the cold temperatures and designed to use battery power for over 10 months of each year without manual maintenance. To minimize power consumption, our system was configured to measure CO_2 concentrations for only 1.5 h day^{-1}. To maintain long-term observations, the operational system included an auto-charging system for 100 batteries and a satellite communication system. Since 2009, we have successfully obtained CO_2 data using this system on Mt. Fuji.

In this paper, we evaluate the system performance (stability and sustainability in operation) in addition to the analytical viewpoint of repeatability and accuracy of the measurements. We present our data for CO_2 concentration at the summit of Mt. Fuji for 6 years and characterize the concentration variation in relation to regional air masses, comparing our data with those from the Mauna Loa Observatory (MLO), Hawaii, and other datasets.

2 Methods

2.1 Location

Mt. Fuji is the highest mountain in Japan, located in the middle of mainland Japan (35.21° N, 138.43° E, 3776 m a.s.l.) on the Pacific side and isolated from other mountain ranges (Fig. 1). It has not erupted since 1707, and no gas emission from the crater has been observed at the mountain summit. There is a small outer rim (200 m height, 800 m diameter) surrounding the crater at the top, with no vegetation above 2500 m. At the summit, the coldest daily temperature observed was −35 °C in February 1981. The maximum daily temperature is about 17 °C in August. There is generally a strong wind, which averages about 12 m s^{-}1; during the passage of a typhoon, wind speed can peak at > 70 m s^{-1}.

The first weather station on Mt. Fuji was constructed on the edge of the highest outer rim at Kengamine in 1936. In 1970, the old building was replaced by the present buildings. Until October 2004, four officers of the JMA stayed for 3 weeks at a time, collectively working throughout the year to make weather observations. Compared to other high-altitude stations such as the MLO in Hawaii and Jungfraujoch in Switzerland, the station at Mt. Fuji is more difficult to access because vehicular transportation is not available. In 2004, manual observations stopped because of the termination of radar observations in 1999 and the change in the role of weather observations at Mt. Fuji due to new technology, including automated weather observations and satellites. After that, a non-profit organization (NPO) started to rent the Mt. Fuji weather station and has managed it for scientific research since 2007.

Currently the Mt. Fuji station is open only in July and August for several proposed research activities (http://npo.fuji3776.net/) and for the maintenance of weather instruments; the NPO provides some staff at the station. Commercial electricity is provided only during this period for safety reasons, because there are no workers on site during the rest of the year. Our measurement system was installed in the third building of the station on 20 July in 2009. Because it includes several instruments, insulation boxes, and batteries (about 3 t total), we asked to use a specialized bulldozer for transportation. We can only access the station during summer for the installation and maintenance of the system and to exchange our standard gas cylinders and other items.

2.2 Measurement system

Figure 2 shows the CO_2 measurement system, a schematic of the gas and the electricity flows, and the insulation method for the main measurement component. The system consists of the main measurement component, power control devices for battery charging and power switching, and 100 shielded lead acid batteries (12 V; G42EP: Enersys Co. Ltd.; service temperature ranges from −40 to 80 °C). The main measurement component (CO_2-MTF1, Kimoto Electric Co. Ltd.) includes a non-dispersive infrared sensor (NDIR; Li-840, LI-COR Co. Ltd.), air pumps (CM-15-12: E. M. P-Japan Ltd.; 1.2W), a drying system using a membrane (Flemion: SWG A01-18: AGC Engineering Co. Ltd.), and a desiccant (Silica gel; 2000 mL). Each device in the measurement component was selected for minimal electricity consumption.

The main measurement component (30 × 30 × 30 cm) was covered with foam insulation (Phenovaboard: Sekisui Chemical Co. Ltd.) and placed in a 100 L plastic insulated box (RPS-100NF: REMACOM Co. Ltd.), which was additionally covered with 15 cm thick Phenovaboard. The temperature at the summit of Mt. Fuji drops below −20 °C in winter. Although the control circuit boards had been tested under such low temperatures in the laboratory, the Li-840 sensor requires a certain temperature (50 °C) in the Li-840's cell when starting the measurements. Furthermore, the diaphragm rubber (chloroprene) of the air pumps could be damaged at such low working temperatures. Therefore, the main measurement component was specially insulated to maintain a suitable working temperature and to save energy for starting the Li-840. In addition, when the temperature of the measurement component falls below 0 °C, a small internal heater maintains the temperature above 0 °C when the pumps start. Each battery was wrapped in plastic film and placed in a corrugated cardboard box, which itself was wrapped in plastic film in case of liquid leakage and for heat insulation.

An air inlet was mounted on a water tank (about 3 × 4 × 3 m), which was located just next to the third building of the station. The water tank was partly covered by wooden boards for protection from snow but with sufficient space for air to penetrate between the wooden cover and the tank. If the air inlet had been placed completely outside, it would have been difficult to take in air during the winter because snow would cover the whole inlet. Air was drawn from the air inlet through about 20 m of 1/4 in. polytetrafluoroethylene (PTFE) tube with a 7-micron filter (Swagelok SS-4F-7) to the station by an air pump with a flow rate of about 1.5 L min^{-1}. In general, metal tubing such as stainless steel or aluminum is better than PTFE for measuring CO_2. However, because the tube was installed outside (between the water tank and the third building), it has to be inconspicuous or transparent because Mt. Fuji is a national park and installation of artificial things is strictly limited by law. Therefore, we selected a transparent PTFE tube but used a slightly higher flow rate for pumping air to minimize contamination from the material. We conducted a leak check every summer and replaced the inlet filter. We also placed a data communication antenna (AT1621-142W-THCF- 000-00-00-NM: AeroAntenna Technology Inc., Chatsworth, CA, USA) for the Iridium satellite (Iridium 9601: KDDI Co. Ltd.; 7.5 W max) in the small space within the wooden cover of the water tank. We constructed two sets of the main measurement component, which were switched each summer after 1 year of operation; the non-operational pumps and other

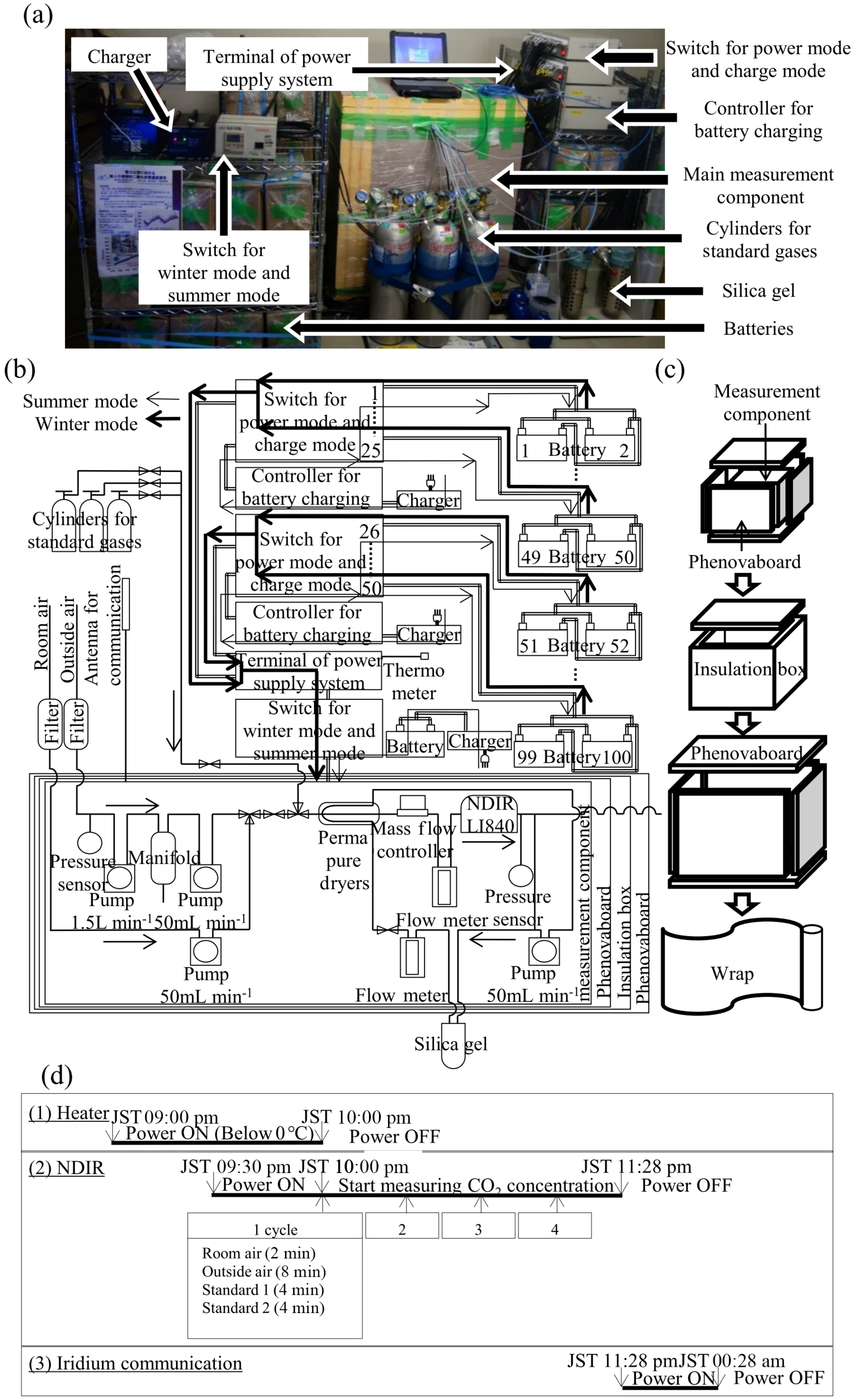

Figure 2. The CO_2 measurement system: **(a)** picture of the system installed in the third building at the Mt. Fuji station, **(b)** schematic of gas and electricity flows. The thin lines and arrows show the direction of electric current in the summer mode, and the thick lines and arrows show it in the winter mode. **(c)** Insulation method used for the main measurement component, and **(d)** measurement sequence.

equipment were then readied for their next deployment the following year.

2.3 Electrical power system

The electrical power line to the station, which runs from the foot of Mt. Fuji, is fairly old as it was mainly installed more than 40 years ago. Furthermore, since the power cables are buried in volcanic rocks which can easily collapse during avalanches, the cables are likely to be damaged. Therefore, at the beginning of every summer, the power line has to be checked and repaired prior to use.

It is too difficult to construct wind turbines or solar panels outside the station under the legal limitations of the national park and the harsh natural conditions at the summit. At present, only a few small solar panels are installed in a limited space for weather observation. Therefore, we needed another electrical source, like batteries, which could operate the measurement system for the remaining 10 months. We investigated two types of battery, lithium and lead acid; the latter was more reliable for autonomous operation. According to the electrical power needed for the system, we decided to use 100 batteries (12 V/G42EP) specially suited for the cold environmental conditions.

These batteries were connected in parallel, and the voltage was automatically checked when the measurement system started. When the voltage was below 10.5 V, the system halted operation to protect the batteries. The electrical power system has a device to switch from "winter mode" to "summer mode". In winter, we used the 100 batteries for powering the system, whereas in summer we used another battery connected to a battery charger powered via the commercial supply (see Fig. 2b).

In summer (July–August), the 100 batteries (two series of 50 batteries) were charged by two specially designed charging controllers. After the battery connection is changed from "power mode" to "charge mode", each controller starts charging a pair of batteries. Normally, each controller can charge 50 batteries, one pair after another, within a 3-week period. At the end of August, the power system was switched to winter mode, and the system operated using the 100 batteries until the following July.

2.4 Measurement sequence

Because of the limited power supply during winter, the measurement system was configured to operate for only about 3.5 h day^{-1} (in addition, measurements are only taken during 1.5 h day^{-1}). We initially selected the time period 14:00–17:28 Japan Standard Time (JST) from 20 July 2009 to 19 July 2010. However, we subsequently changed the operational time to 21:00–00:28 JST, to avoid local daytime influences from transportation of the air mass around Mt. Fuji that might affect the CO_2 concentration over the summit; this is similar to how baseline condition is obtained at MLO.

The measurement sequence is summarized in Fig. 2d. The sequence is controlled by the control board (MC-mini, Kimoto Electric Co. Ltd.). Briefly, at 21:00 JST, the temperature of the measurement system is checked and the heater operates for an hour if the temperature is less than 0 °C. The Li-840 starts at 21:30 JST and the cell temperature increases to about 50 °C within 30 min (14 W max). Then, starting at 22:00 JST, room air is introduced into the Li-840 (3.6 W) for 2 min using a small pump with a flow rate of 50 mL min^{-1}. This process is intended to purge the inside measurement line with new room air and stabilize the conditions (e.g., the temperature and drying system) before outside air is introduced. During this time outside air is drawn into a manifold by a medium-volume pump at a flow rate of 1.5 L min^{-1}. Then, an aliquot of just 50 mL min^{-1} is introduced into the drying and measurement system regulated by a mass flow controller for 8 min. Next, three working standard gases (about 360, 390, and 420 ppm in a 10 L aluminum cylinder), prepared by the Japan Fine Products Co. and calibrated against the NIES09 CO_2 scale (Machida et al., 2009), are measured for 4 min each to calibrate the system. Generally, this sequence is repeated four times. According to the results of the sixth World Meteorological Organization (WMO)/International Atomic Energy Agency (IAEA) Round Robin intercomparison (NOAA/ESRL, 2016), we know the scale difference between NIES09 and NOAA. Although the NIES09 scale was lower than the NOAA scale by 0.04–0.09 in a range of 376–404 ppm, both scales are fairly close to each other. We used special regulators (TORR-1300: Nissan Tanaka Co.) which are able to work stably within 15 % deviation at the 0.1 MPa level even in a large temperature range from −25 to 50 °C.

At 23:28 JST, the Iridium satellite data communication is activated for 1 h until the data (192 bytes) are sent successfully. Communications become difficult under bad weather conditions, such as cloud cover at the summit, so the 1 h period allows for reliable data communication. If data cannot be sent at that time, the device tries again the next day. Actually, in 2009–2010 we used ORBCOMM satellite communication, but because of poor transmissions we changed to Iridium.

In addition, data were stored as 10 s averages to a CompactFlash (CF) card in the system. The derived concentration was based on the average of the data from the second, third, and fourth cycles; in other words, the daily average is based on 3×6 min (because we discarded the first 2 min data for 8 min data) = 18 min of observations.

2.5 Continuous measurement in summer and flask sampling

Because this system monitors CO_2 mole fraction only for a short period (22:00–23:28) of the day, we needed to evaluate the daily variation of CO_2 concentration to clarify how this measurement represents the CO_2 concentration over Mt.

Fuji. In the summers of 2012 and 2013, we set up a simple continuous CO_2 measurement system, connected to the inlet line of the measurement system. It comprises a second Li-840, flow-adjusting parts, a gas selector, and four standard gases (NIES09 CO_2 scale). Although this system has no drying component, the dry air base CO_2 mole fraction is calculated from the H_2O concentration measured by the Li-840 itself with a good repeatability (below 1 %); the repeatability of the CO_2 measurement was found to be better than 0.3 ppm (signal-to-noise ratio was below 0.1 ppm), which is sufficient to evaluate the CO_2 daily variation.

Furthermore, to evaluate the accuracy of the measurement system, we compared the CO_2 mole fraction between the battery-powered measurement system and flask samples analyzed later in the laboratory. Air was collected by 1.5 L glass flask four times per year (12 times in total) during July and August 2009–2011 near the inlet of the battery-powered measurement system when the system measured CO_2 mole fraction. This flask sampling was done by pumping through the glass flask with a small air pump for about 10 min with a flow rate of about 2 L min^{-1} and shutting both inlet and outlet valve after stopping the pump. So, the pressure in the flask was about 650 hPa. By the end of the summer season, we brought the flask to the laboratory in NIES and analyzed the CO_2 mole fraction by NDIR (Li-7000, LI-COR Co. Ltd.) with a metal bellows pumping system (MB-21, Senior Aerospace Metal Bellows) to send air in the flask to the NDIR.

2.6 Other datasets of CO_2 data

For comparison with the Mt. Fuji CO_2 data, we obtained daily data from the MLO, which is located at a similar altitude (19.54° N, 155.58° W, 3397 m a.s.l.; Tans and Keeling, 2016; www.esrl.noaa.gov/gmd/ccgg/trends/). We also used data from aircraft measurements obtained via the Comprehensive Observation Network for Trace Gases by Airliner (CONTRAIL) project (Machida et al., 2008). We selected CONTRAIL data over Japan in the region 34–36° N, 136–141° E at an altitude of 3600–3900 m during 2009–2013. The CO_2 concentration trend was calculated according to the method of Thoning et al. (1989) with a cut-off frequency of 667 days (0.5472 cycles yr^{-1}) for a fast Fourier transform filter.

2.7 Weather data

The temperatures in the room and inside the measurement system were monitored by the system itself, while the system measured CO_2 concentration from the outside air. The external temperature at the summit of Mt. Fuji was measured by the JMA, and the data were taken from the JMA website (http://www.data.jma.go.jp/obd/stats/etrn/index.php).

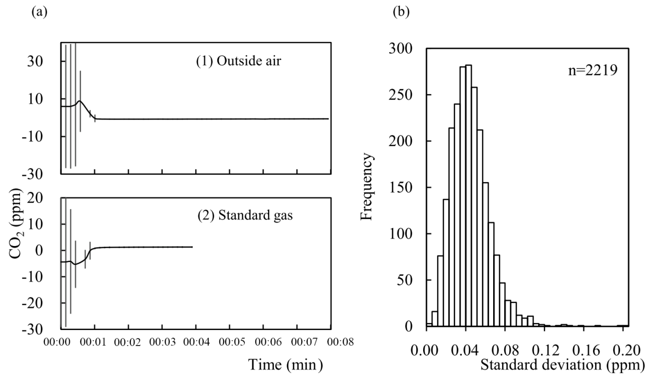

Figure 3. (a) The difference in CO_2 concentration for (1) outside air and (2) standard gas, between the individual measurement values (averaged for 10 s) and over the entire measurement periods, and **(b)** standard deviation of standard gas measurement values during 2–4 min.

2.8 Backward-air-trajectory analysis

In order to assess the sources for regional air masses affecting the station, we calculated backward air trajectories using the METEX system (Zeng and Fujinuma, 2004) available via the website of the Center for Global Environmental Research, National Institute for Environmental Studies (http://db.cger.nies.go.jp/metex/trajectory.jp.html). METEX uses horizontal and vertical wind speed from European Centre for Medium Range Weather Forecast (ECMWF) analyses on a 0.5° × 0.5° mesh to calculated 72 h trajectories.

3 Results and discussion

3.1 Analytical performance of the system at the station

CO_2 data from the Li-840 were recorded every 1 s and averaged over 10 s. Signals from the Li-840 for the outside air and the working standard gases are shown in Fig. 3a. The data of the first 2 min had high variation because of the purging and exchanging of air during this period, so we discarded the data of the first 2 min and averaged the rest. The standard deviation of measurement values for the working standard gas is shown in Fig. 3b. The noise level for 2 min averages of this system was usually lower than 0.1 ppm.

The calibration using three working standard gases was done repeatedly every day. These working gases were calibrated by our NIES calibration system in the laboratory with a high accuracy below 0.1 ppm, which was confirmed by a WMO/IAEA Round Robin inter-comparison. Certified values for the standard gases prior to use and after use (i.e., 2–3 years later) are shown in Table 1. Because the standard gas was pressurized in relatively small cylinders (i.e., 10 L aluminum cylinder), the drifts in CO_2 concentration over 2–3 years were relatively large. However, their values still

Table 1. Location of Mt. Fuji (35.21° N, 138.43° E) and of other sites representative for the long-term observation of atmospheric CO_2 concentration in Japan (small black dots), and the five areas used for back-trajectory analysis of air mass origins (Siberia, China, Southeast Asia, around Japan, and Pacific Ocean).

	Before the cylinder installation				After the cylinder replacement				Change of concentration	
Cylinder no.	Date of calibration	Calibrated value (ppm)	Pressure of cylinder (MPa)	Date of installation	Date of replacement	Date of re-calibration	Re-calibrated value (ppm)	Pressure of cylinder (MPa)	Change amount of the concentration (ppm)	Change rate (ppm yr^{-1})
CPC-00449	17-Jun-2009	368.86	10.8	16-Jul-2009	24-Jul-2011	19-Aug-2011	368.82	3.4	−0.03	−0.02
CPC-00447	17-Jun-2009	383.10	11.0	16-Jul-2009	24-Jul-2011	19-Aug-2011	383.24	4.0	0.14	0.06
CPC-00448	17-Jun-2009	403.45	10.8	16-Jul-2009	24-Jul-2011	19-Aug-2011	403.54	3.2	0.09	0.04
CPC-00445	10-Jun-2011	367.94	11.4	25-Jul-2011	25-Jul-2013	6-Aug-2013	368.02	0.8	0.09	0.04
CPC-00450	10-Jun-2011	383.46	11.5	25-Jul-2011	25-Jul-2013	6-Aug-2013	383.42	3.6	−0.04	−0.02
CPC-00451	10-Jun-2011	402.29	11.5	25-Jul-2011	25-Jul-2013	6-Aug-2013	402.37	3.4	0.08	0.04
CPC-00043	23-Jun-2013	367.10	12.8	26-Jul-2013	1-Jul-2016	10-Jul-2016	367.12	2.5	0.02	0.01
CPC-00448	23-Jun-2013	393.17	12.6	26-Jul-2013	1-Jul-2016	10-Jul-2016	393.12	2.5	−0.05	−0.02
CPC-00449	23-Jun-2013	418.59	12.8	26-Jul-2013	1-Jul-2016	10-Jul-2016	418.44	2.5	−0.15	−0.05
CPC-00445	15-Jun-2016	389.18	13.2	2-Jul-2016						
CPC-00450	15-Jun-2016	409.15	13.2	2-Jul-2016						
CPC-00451	15-Jun-2016	429.16	13.2	2-Jul-2016						

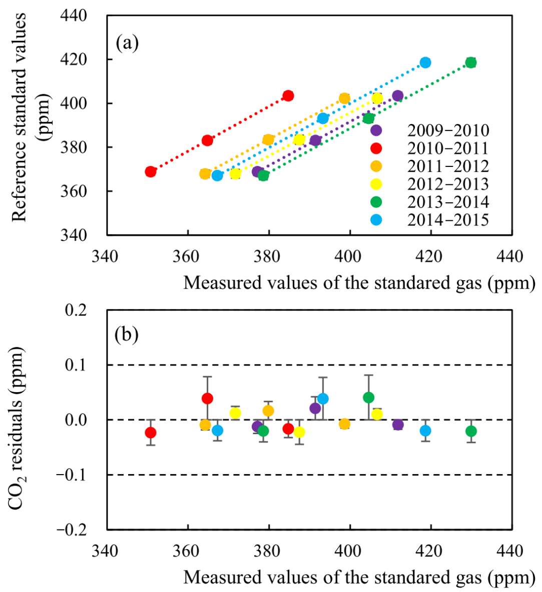

Figure 4. (a) Linearity tests between the apparent measured values of the standard gas and the reference standard values (assigned values), and **(b)** CO_2 residuals.

showed sufficient concentration stability, mainly better than 0.1 ppm.

Calibration curves using these standards, as measured by the system, are shown in Fig. 4a. Because the main measurement unit was exchanged every year and standard gas series were changed every 2 or 3 years, apparent output values measured and corresponding calibration curves were different in each year. Since the span of the Li-840 was rather stable, calibration curves were also stable during a year. The calibration curve was made by linear regression for simplicity. Figure 4b shows the difference between the assigned values of standards and calibrated values for each calibration curve made by the system. Calibration was done four times a day, and the differences in each calibration curve were averaged over 1 year; the standard deviations were also calculated and plotted. Deviations from the calibration curve were fairly small (lower than 0.05 ppm), and their variations were also smaller than 0.05 ppm, suggesting that measurements were sufficiently precise in accordance with WMO recommendations for this period.

Every summer we replaced the inlet filter and drying cartridge of silica gel in addition to exchanging the main measurement unit. There was no problem with filtering and drying the air during any 1 year of operation. Over 90 % of the silica gel was still blue after 1 year, indicating it had not been exhausted. As mentioned in the experimental section, pumps installed in the system were replaced by new ones annually and also worked properly.

Daily summary data transmission by Iridium was also done automatically. We found that bad weather conditions (clouds and rain) sometimes influenced the success ratio of satellite transmission. During the rainy season from June to July, the success ratio was 0.4–0.5. During poor weather, the system attempted communication with the satellite at least twice a day on average to send daily data. For other months the success ratio was as high as 0.6–0.7. When using the ORBCOMM satellite, the ratio was lower than 0.2; it was harder to send data and caused extra power consumption, although all the data could be stored on a CF card. Therefore, the Iridium communication system we subsequently adopted seemed better for sending our data.

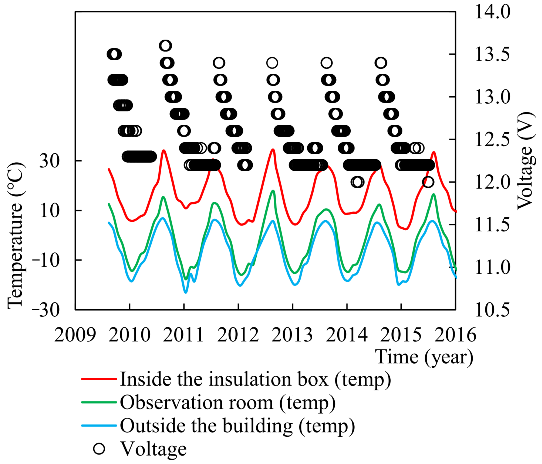

Figure 5. Daily averages of ambient temperatures outside the building, within the observation room, and inside the insulation box, along with daily voltage readings for the batteries. Temperatures inside the insulation box and observation room were measured by the CO_2 measurement system at the same time that atmospheric CO_2 concentrations were measured. The temperature outside the building was measured by JMA; data were taken from the JMA website (http://www.data.jma.go.jp/obd/stats/etrn/index.php). One hundred batteries (12 V) were connected in parallel, and the voltage was checked when the measurement started.

3.2 Operation with 100 batteries over 6 years

The total power consumption of the CO_2 measurement system was estimated to be about 3 A for 3 h day^{-1}. However, if a single battery can last 42 ampere hours (Ah), then 100 batteries could operate for 467 days under ideal conditions. As mentioned earlier, however, the ambient temperature on Mt. Fuji is low in winter and so reduces battery capacity. In addition, the operation of the small heater in the system shortens the duration of operation further.

Figure 5 shows daily data for the outside temperature on Mt. Fuji, within the observation room, and within the measurement system protected by the insulation box. The outside temperature was very low until April, sometimes below −20 °C. The average temperature in January was −19.8 ± 4.4 °C. The room temperature (−15.4 ± 1.9 °C) was about 5 °C higher than the outside temperature.

The temperatures of the batteries were similar to the ambient temperature, which have affected their capacities. On the other hand, the temperature inside the insulation box was 15 °C higher than the room temperature. Even in winter, the average temperature of the system remained just above 0 °C because small amounts of heat were produced by each device (e.g., the pump, circuit board, and Li-840 sensor) during the operational time, which was retained within the insulated box. Consequently, the system's small heater rarely operated in winter. The CO_2 measurement system was able to measure CO_2 concentrations stably in spite of the low-temperature conditions.

Figure 5 also shows the voltage of the batteries during the operation. The voltage just after charging in summer was 13.4–13.6 V but decreased gradually to 12.0–12.2 V by July of the following year. After March, the voltage seemed to recover as the temperature increased toward summer. Over the 6-year period, voltages less than 10.5 V were not observed. Therefore, measurements of CO_2 concentration were not interrupted by power shortages. In terms of battery condition, the G42EPs were very stable even though they were used for over 6 years, although the lowest voltage decreased from 12.3 to 12 V. The automatic charging system was very effective with respect to simplifying maintenance, as it could charge all batteries within 3 weeks. Thus, we concluded that our CO_2 measurement system, developed for the specific conditions of Mt. Fuji with its harsh weather and limited power supply, operated successfully for 6 years with no interruptions except for short periods of maintenance during summer. In total, we recorded 2219 days of data from July 2009 to December 2015 (a total of 2354 days), which corresponds to 94 % of the period.

At the station, we often observed lightning in the summer. To prevent severe damage of the instruments at the station by voltage spikes conducted through the power cable, the Mt. Fuji weather station sometimes (once or twice per summer season) stopped grid electricity and changed the source to a small generator at the station. At such times, our charging system stopped and waited for the recovery of the grid electricity before restarting automatically. On two occasions, the operation of the system was interrupted by damage to a power board in the main control unit because of lightning (2 April–23 July 2012 and 1–18 August 2014). Particularly in the summer season, there are often thunderstorms observed at the summit because the station is in the cloud layer. Recently, we connected a new ground line between the observation building and the water tank facility to reduce the risk of lightning passing through the Iridium antenna cable. However, we are still unsure whether this will be sufficient to mitigate the risk of a lightning strike affecting the measurement system.

3.3 Evaluation of the sampling time in terms of the daily variation of CO_2 concentration at the summit of Mt. Fuji

The CO_2 concentrations at the summit of Mt. Fuji were observed continuously in the summers (July–August) of 2012 and 2013. Figure 6 shows the difference between the hourly and daily averages of CO_2 concentration during the observed periods. The hourly averages of the difference showed random variations within a range of about 0.5 ppm with no clear diurnal variation. In the 2012 data, concentration tended to decrease slightly (less than 0.4 ppm) before noon, although this tendency was not seen in 2013. At the MLO, afternoon

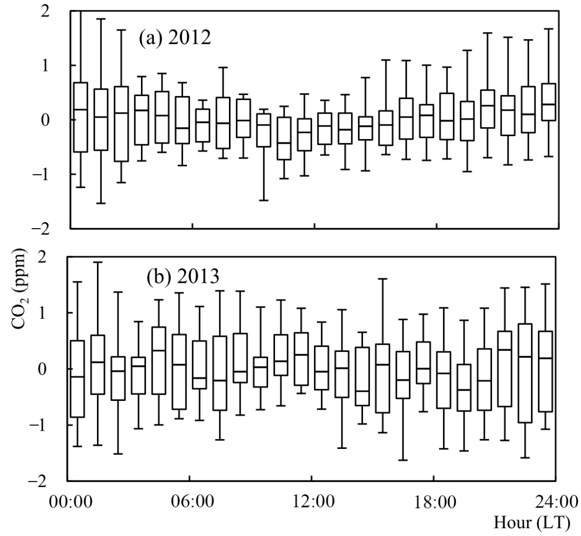

Figure 6. Difference between hourly average and daily average CO_2 concentration during the observed periods: **(a)** 2012 and **(b)** 2013. Median value (the line in the box), inner 50th percentile of the value (box), and inner 95th percentile of the value from the daily average for each hour of the day for the CO_2 mixing ratio at Mt. Fuji.

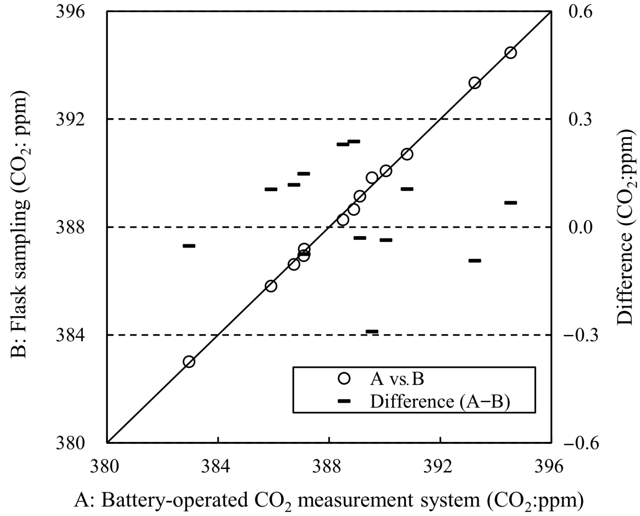

Figure 7. Comparison between CO_2 concentrations measured by the battery-operated CO_2 measurement system and in the flask-sampling experiment, and the difference in CO_2 concentration between both results.

data are usually excluded because they include vegetation effects. However, since no clear diurnal cycle could be observed, we conclude that the timing of the air sampling at Mt. Fuji did not affect the monthly and yearly averages. Although the sampling time was changed from daytime to nighttime in July 2010, we believe that this change did not affect the results of the trend analysis. Nakazawa et al. (1984) and Sawa et al. (2005) also reported that daily variation of CO_2 concentration at the summit of Mt. Fuji was very small. Tsutsumi et al. (1994) observed O_3 concentration at the summit of Mt. Fuji and reported that the small daily variation observed was influenced by a mountain–valley wind system in summer; however, the variation was much smaller than at MLO, Niwot Ridge in the USA (40.05° N, 105.59° W, 3528 m a.s.l.), and Hakkoda (40.41° N, 140.51° E, 1324 m a.s.l.) in Japan. Igarashi et al. (2004) observed SO_2 variation at the summit of Mt. Fuji, and although they did not find any daily variation, they did reveal episodic large-distance transport from the Asian continent. According to observations at the summit of Mt. Fuji by Sawa (2005), the short-term cycle of CO concentration variation was related to neither wind direction nor wind velocity, though its variation was considered to be affected by regional-scale pollution over Asia. Thus, the elevation of an observing station must be sufficiently high to minimize surface influences from local pollution and vegetation.

3.4 Comparison with the flask sampling data and aircraft measurements over Japan

In general, even if measurements are thoroughly calibrated, biases cannot always be excluded, for example due to leaks in the sampling line or other measurement issues. To assess the accuracy of our measured CO_2 values, we therefore conducted comparison experiments using flask sampling and analysis. The air was collected into a glass flask at the same time as the measurement system worked at the summit, usually during daytime in the summers of 2009–2011. For this comparison, we ran the measurement system four times a day, including periodical timing.

CO_2 values from the system were very similar to those collected by the flask sampling experiment (Fig. 7). The mean differences were almost zero (0.04 ppm) with a standard deviation of 0.15 ppm. The variations were partly caused by our sampling method for glass flasks, which only provided low atmospheric pressure of the air in the flask, making the analytical precision worse sometimes. Thus, we conclude that our measurement system could measure CO_2 mole fraction fairly accurately.

To study how well our CO_2 data represented regional characteristics around Japan not only in summer but over the whole year, we also compared them to data observed by the CONTRAIL project. We selected CONTRAIL data, taken on the same day as our measurements, within the region 34–36° N, 136–141° E, at altitudes of 3600–3900 m during 2009–2013. Multiple daily points were averaged as daily data.

Figure 8 shows a scatterplot between both datasets. The data scatter around the 1 : 1 line, and the average differ-

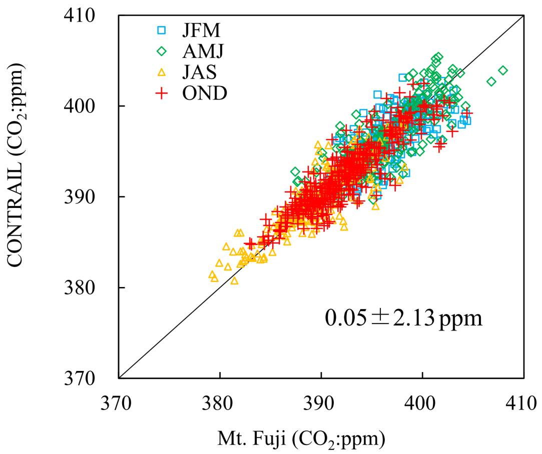

Figure 8. Scatterplots of CO_2 concentration at Mt. Fuji and obtained by CONTRAIL.

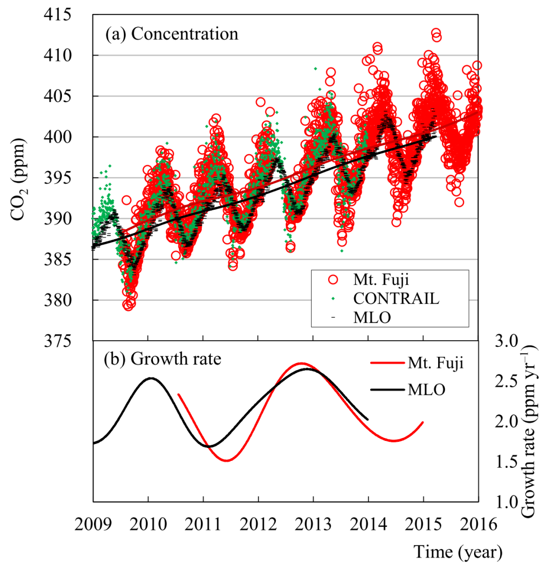

Figure 9. (a) Daily average of CO_2 concentration and the trend of CO_2 concentration (solid line), and **(b)** growth rates for data from Mt. Fuji, CONTRAIL, and Mauna Loa Observatory (MLO) 2009–2015. Atmospheric CO_2 concentration at Mt. Fuji was measured at 22:00–23:28 JST, compared with the daily average of atmospheric CO_2 concentration for CONTRAIL and MLO data. CONTRAIL data were selected over Japan in the region 34–36° N, 136–141° E at an altitude of 3600–3900 m during 2009–2013, and Mauna Loa Observatory is located at a similar altitude (19.54° N, 155.58° W, 3397 m a.s.l.).

ence was only 0.05 ± 2.13 ppm. On average, the datasets thus show good agreement, but the standard deviation is relatively large. This is likely influenced by the difference in the measuring time, as our measurements were taken at night and CONTRAIL's were taken throughout the day, and by the variable distance from Mt. Fuji. It is not straightforward to compare these data directly given such differences in spatial and temporal sampling. However, Fig. 8 suggests that the concentrations in both datasets are highly consistent on average, implying that our dataset was showing regionally representative CO_2 concentration. Therefore, we conclude that the summit of Mt. Fuji can be considered a suitable location for sampling free-tropospheric air over the Eastern Asian region throughout the year, unaffected by local wind blowing from the valley around the Mt. Fuji weather station.

3.5 Effects of air mass origin on seasonal variation in CO_2

Observations of CO_2 mole fraction measured at the summit of Mt. Fuji (2009–2015) are plotted together with daily data from CONTRAIL and MLO in Fig. 9 (monthly average data are shown in Supplement Table S1; daily data will be shown on a website: http://db.cger.nies.go.jp/portal/overviews/index?lang=eng). A seasonal minimum clearly occurs in September and a maximum in April or May, though local minimum concentrations (episodic low concentration) were often seen in July. The seasonal amplitude of variation at Mt. Fuji was the same as the amplitude in the CONTRAIL data and about 18 ppm higher than the amplitude at MLO (8 ppm). In general, the seasonal amplitude of CO_2 variation is greater over land areas than oceanic areas because of the influence of photosynthesis and respiration of local and/or regional vegetation, and anthropogenic CO_2 emissions.

Japan has a seasonal wind pattern (i.e., the monsoon), and the CO_2 concentration must be affected by the wind direction and the origin of the air mass. To clarify the characteristics of the seasonal variation of CO_2 concentration at Mt. Fuji, we plotted the difference between the daily concentration at Mt. Fuji and MLO (ΔCO_2) in Fig. 10. The CO_2 concentration levels at both stations were similar from July to September, when oceanic air prevails over Japan, although occasional lower concentrations occurred in July at Mt. Fuji. Conversely, the CO_2 concentration from December to March at Mt. Fuji was generally higher than at MLO.

To characterize the difference between the two sites, we performed a trajectory analysis for the daily data obtained at Mt. Fuji. We divided the surrounding region into five areas (Siberia, China, Southeast Asia, Pacific Ocean, and around Japan) of air mass origins according to a 72 h trajectory analysis, as shown in Fig. 1. The distribution of the air mass origins showed clear differences in each season. In the summer air masses came from various areas, but in winter air masses mainly originated from China and in some cases from Siberia and Southeast Asia. The ΔCO_2 concentrations for June–August and January–March are shown in Fig. 11 for the five areas of origin. Siberian air masses always carry lower concentrations than the background air arriving at MLO. In addition, Chinese air sometimes (three or four times per season) had much lower concentrations than Siberian air (i.e., up to 10 ppm less), but it also sometimes (once per season)

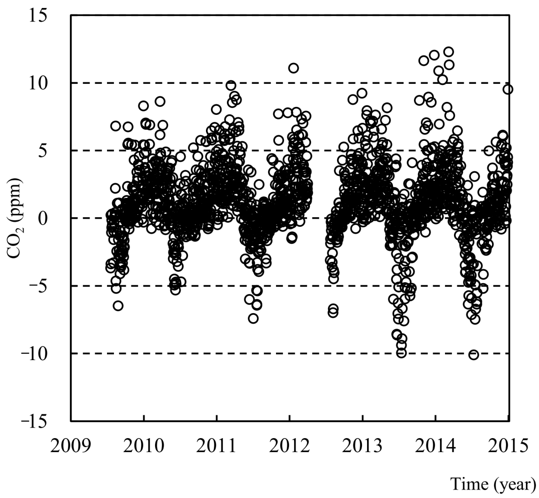

Figure 10. Difference between daily CO_2 concentrations at Mt. Fuji and Mauna Loa Observatory, 2009–2014.

had concentrations up to 7 ppm higher than at MLO in summer. Such characteristics might be explained by CO_2 uptake by the vegetation of Siberia and China and by CO_2 addition from anthropogenic emissions over the Asian continent. Conversely, air originating from the Pacific Ocean and the areas near Japan and Southeast Asia showed similar concentrations to MLO. Therefore, we concluded that lower summertime CO_2 concentrations (compared to MLO) were related to the origin of the air mass, especially those from Siberia and China, which are influenced by terrestrial ecosystems.

In winter, air from all areas except the Pacific Ocean showed higher concentrations than at MLO, indicating some influence from the continent, or even Southeast Asia. In particular, air originating from China sometimes (three or four times per season) showed much higher concentrations than air from other areas, suggesting that anthropogenic CO_2 was added to the air over China in winter. In addition, this season corresponded to the season of biomass burning on the Indochinese Peninsula (Sawa, 2005), which may also influence this higher concentration for the Southeast Asian sector.

Sawa et al. (2005) reported that CO_2 concentrations at Mt. Fuji were 2 ppm lower than the level at Minamitori Island in summer but 3 ppm higher in winter; this island is located 2000 km southeast of Mt. Fuji and 5000 km west of MLO (Watanabe et al., 2000). They stated that the air mass over Mt. Fuji must be influenced by continental air. Similarly, at Hateruma Island, which is much closer to China, the influence from the continent was clearly observed, especially in winter (e.g., Tohjima et al., 2010).

Overall, the seasonal variation of CO_2 concentration at Mt. Fuji was characterized by values lower than MLO in summer, associated with air carried from Siberia and Asia in summer, and values higher than MLO in winter, associated with air from China which is influenced by emissions over the Asian continent.

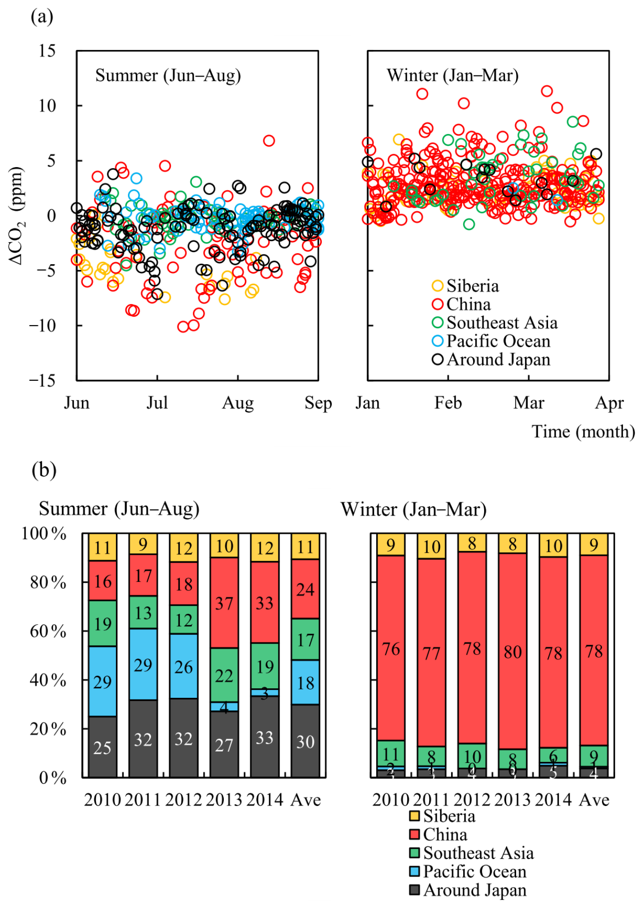

Figure 11. (a) Differences between daily CO_2 concentration in summer (June–August) and winter (January–March) at Mt. Fuji and Mauna Loa Observatory for five areas of air mass origin (Fig. 1), and **(b)** percentage of air mass origin in summer (June–August) and winter (January–March) at Mt. Fuji from 2010 to 2014.

The yearly variation in seasonal characteristics of CO_2 concentration shown in Fig. 10 also revealed some interesting tendencies. For example, the negative values of ΔCO_2 concentration in summer (June–August) became especially large in 2013 and 2014. Looking at the air masses shown in Fig. 11b, the frequency of air masses originating from China increased in these 2 years, while the Pacific Ocean decreased its ratio. Accordingly, ΔCO_2 became relative low in 2013 and 2014 because air masses originating from Siberia and China carried relatively low CO_2 concentrations.

3.6 Trend analysis

Nakazawa et al. (1984) and Sawa et al. (2005) reported that CO_2 mole fraction on average was 337.8 and 338.8 ppm in October 1980 and 1981, respectively, and 374.8 ppm in October 2003. Therefore, the CO_2 concentration at the summit of Mt. Fuji increased by as much as 62 ppm over the 35 years from 1980 to 2015. We calculated the annual rate of increase since 2009 as 1.5–2.7 ppm yr^{-1} (Fig. 9). This was reasonably matched with the growth rate at MLO (Tans and Keeling, 2016). These rates were slightly higher than those in the 1980s (1.0–2.3 ppm yr^{-1}), because anthropogenic CO_2 emissions have increased to > 10 Gt-C yr^{-1} in recent years, while they were only as high as 5 Gt-C yr^{-1} in the 1980s (Le Quéré et al., 2015). In particular, higher growth rates were observed in 2010, 2012, and 2015. In general, El Niño years lead to a higher global surface temperature, which is connected to an increased rate of growth of CO_2 because of accelerated plant respiration over land, weakened photosynthesis activity, and occurrence of biomass burning (van der Werf et al., 2008). However, 2012 was exceptional as it was not an El Niño year. As for 2015, a clear El Niño occurred and frequent biomass burning events were observed especially in Southeast Asia, so the increase growth rate toward 2015 was reasonable.

These recent growth rate variations were almost the same as at MLO, suggesting that the long-term stability for our CO_2 observation system is reliable. However, the trend line itself (average concentration) was higher at Mt. Fuji than that of MLO. As mentioned in the last section, because of influences by the wind patterns and air mass origins, the annual average concentration at Mt. Fuji was about 1 ppm higher than MLO. Therefore, the trend line of Mt. Fuji exceeded 400 ppm around October 2014, while MLO exceeded this mark in March 2015, as shown in Fig. 9.

4 Conclusions

We developed a battery-powered CO_2 measurement system and installed it in 2009 at the weather station on the summit of Mt. Fuji, where there is no grid-based electricity from September to June. This system has reliably observed year-round atmospheric CO_2 mole fractions from 2009 to 2015, except for brief interruptions due to lightning damage; CO_2 data were obtained for 94 % of all days of the observation period. We improved the lightning countermeasures by grounding between the buildings, but safer technology may be needed to prevent lightning incidents from disrupting future longer monitoring periods.

For sustainable and easy operation, we also developed an automatic battery-charging system, which could charge all 100 batteries automatically within 3 weeks. This was essential for continuous observations at Mt. Fuji, because researchers cannot stay at the station during the 3-week charging period. The performance of these batteries was still good after 6 years. In the near future, however, we plan to replace the batteries with new ones.

Even though the room temperature declined to −20 °C in winter, the system worked properly. The insulation box kept the main unit warm enough and the pumps worked safely for 1 year at a time; the small heater for increasing temperature rarely needed to operate, helping reduce power needs. Replacing the whole measurement unit and pumps every summer and the maintenance of used pumps were very important for reliable operation during the 10-month winter period when access is not possible. In addition, having an extra unit at hand meant that we could quickly respond to sudden incidents (usually by lightning) and could exchange the system very quickly if these occurred in the summer, like in 2015. The daily satellite data transmission was also successful after changing the system from ORBCOMM to Iridium.

We conclude that our system could measure CO_2 concentration accurately and stably using a calibration strategy with daily calibrations with three working standard gases, which were fairly stable in their concentration for over 2 years. The high accuracy was confirmed by a comparison with independent flask samples collected at the station.

We also compared our measured values of CO_2 at Mt. Fuji with CONTRAIL-derived data and found that both datasets were in good agreement in the area relatively close to Mt. Fuji, despite the inclusion of data obtained around the Tokyo area. This suggested that data obtained at Mt. Fuji were comparable with other background data and that these data could be highly representative. Because of power limitations, the system obtained data only during a limited time period from 22:00 to 23:28. Even so, because daily variation in CO_2 concentration was found to be very small (< 0.5 ppm), our data can be used as a representative daily dataset in this region, as confirmed by the good agreement with the CONTRAIL data.

Historically, CO_2 concentrations at Mt. Fuji have increased by about 62 ppm from 1980 to 2015, similar to MLO. The recent rate of increase in CO_2 concentration was found to be 1.5–2.7 ppm yr^{-1}, also consistent with the rate at MLO. However, there were seasonal differences between the two sites. In summer, the CO_2 concentration at Mt. Fuji is about 2–10 ppm lower than at MLO, whereas in winter the CO_2 concentration at Mt. Fuji is about 2–12 ppm higher. Such differences were related to the large variation in seasonal origins of air masses over Japan as determined by the regional wind patterns.

Even in the same season, CO_2 characteristics depended on air mass origin. For example, air masses originating from Siberia and China in summer showed lower CO_2 concentrations than other origins, while air masses from China and Southeast Asia in winter had relatively high values. Such regional source and sink characteristics could be clearly monitored in the CO_2 concentration at Mt. Fuji, suggesting that the developed system can be applied for long-term regional environmental monitoring.

5 Data availability

We will add digital object identifiers (DOIs) to CO_2 daily data of Mt. Fuji and release those data on our website (http://db.cger.nies.go.jp/portal/geds/atmosphericAndOceanicMonitoring?lang=eng) by 2017.

In order to obtain the data before they are released on the website, please contact us (cgerdb_admin@nies.go.jp).

The Supplement related to this article is available online at doi:10.5194/amt-10-667-2017-supplement.

Competing interests. The authors declare that they have no conflict of interest.

Acknowledgements. We received a great deal of support to the NPO "Valid Utilization of Mt. Fuji Weather station" while we undertook this study at the summit of Mt. Fuji. This work was partly supported by funds (Development for Monitoring Technology Related to Global Warming) from the Ministry of the Environment, Japan. We thank Pieter Tans and the Global Monitoring Division team of the National Ocean and Atmosphere Administration (NOAA) for providing CO_2 data of Mauna Loa Observatory. We also thank the CONTRAIL project team for providing CO_2 data near Mt. Fuji. In addition, we would like to thank K. Kinoshita, K. Maeda, Y. Yamamoto, and T. Kitaguchi in Kimoto Electric Co. for their excellent support in the maintenance of the system.

Edited by: D. Brunner
Reviewed by: M. Steinbacher and one anonymous referee

References

Boden, T. A., Marland, G., and Andres, R. J.: Global, regional, and national fossil-fuel CO_2 emissions, Carbon Dioxide Information Analysis Center, Oak Ridge National Laboratory, US Department of Energy, Oak Ridge, Tenn., USA, doi 10.3334/CDIAC/00001_V2016, 2016.

Conway, T. J., Tans, P. P., Waterman, L. S., Thoning, K. W., Kitzis, D. R., Masarie, K. A., and Zhang, N.: Evidence for interannual variability of the carbon cycle from the National Oceanic and Atmospheric Administration/Climate Monitoring and Diagnostics Laboratory Global Air Sampling Network, J. Geophys. Res., 99, 22831–22855, 1994.

Igarashi, Y., Sawa, Y., Yoshioka, K., Matsueda, H., Fujii, K., and Dokiya, Y.: Monitoring the SO_2 concentration at the summit of Mt. Fuji and a comparison with other trace gases during winter, J. Geophys. Res., 109, D17304, doi:10.1029/2003JD004428, 2004.

Keeling, C. D., Bacastow, R. B., Carter, A. F., Piper, S. C., Whorf, T. P., Heimann, M., Mook, W. G., and Roellofzen, H.: A three dimensional model of atmospheric CO_2 transport based on atmospheric winds (1), Analysis of observational data, in: Aspects of Climate Variability in the Pacific and the Western Americas, edited by: Peterson, D. H., Geographical Monograph, 55, 165–236, 1989.

Keeling, C. D., Piper, S. C., Bacastow, R. B., Wahlen, M., Whorf, T. P., Heimann, M., and Meijer, H. A.: Exchanges of atmospheric CO_2 and $^{13}CO_2$ with the terrestrial biosphere and oceans from 1978 to 2000, 1, Tech. Rep. SIO Ref. Ser., 01–06, 2001.

Le Quéré, C., Moriarty, R., Andrew, R. M., Canadell, J. G., Sitch, S., Korsbakken, J. I., Friedlingstein, P., Peters, G. P., Andres, R. J., Boden, T. A., Houghton, R. A., House, J. I., Keeling, R. F., Tans, P., Arneth, A., Bakker, D. C. E., Barbero, L., Bopp, L., Chang, J., Chevallier, F., Chini, L. P., Ciais, P., Fader, M., Feely, R. A., Gkritzalis, T., Harris, I., Hauck, J., Ilyina, T., Jain, A. K., Kato, E., Kitidis, V., Klein Goldewijk, K., Koven, C., Landschützer, P., Lauvset, S. K., Lefèvre, N., Lenton, A., Lima, I. D., Metzl, N., Millero, F., Munro, D. R., Murata, A., Nabel, J. E. M. S., Nakaoka, S., Nojiri, Y., O'Brien, K., O lsen, A., Ono, T., Pérez, F. F., Pfeil, B., Pierrot, D., Poulter, B., Rehder, G., Rödenbeck, C., Saito, S., Schuster, U., Schwinger, J., Séférian, R., Steinhoff, T., Stocker, B. D., Sutton, A. J., Takahashi, T., Tilbrook, B., van der Laan-Luijkx, I. T., van der Werf, G. R., van Heuven, S., Vandemark, D., Viovy, N., Wiltshire, A., Zaehle, S., and Zeng, N.: Global Carbon Budget 2015, Earth Syst. Sci. Data, 7, 349–396, doi:10.5194/essd-7-349-2015, 2015.

Machida, T., Matsueda, H., Sawa, Y., Nakagawa, Y., Hirotani, K., Kondo, N., Goto, K., Nakazawa, T., Ishikawa, K., and Ogawa T.: Worldwide Measurements of Atmospheric CO_2 and Other Trace Gas Species Using Commercial Airlines, J. Atmos. Ocean. Tech., 25, 1744–1754, doi:10.1175/2008JTECHA1082.1, 2008.

Machida, T., Katsumata, K., Tohjima, Y., Watai, T., and Mukai, H.: Preparing and maintaining of CO_2 calibration scale in National Institute for Environmental Studies-NIES 95 CO_2 scale, proceeding of the 14 the WMO Meeting of Experts on Carbon Dioxide Concentration and Related Tracer Measurement Techniques, in: WMO/GAW Rep., edited by: Laurila, T., 186, 26–29, 2009.

Maksyutov, S., Machida, T., Mukai, H., Patra, P. K., Nakazawa, T., and Inoue, G.: Effect of recent observations on Asian CO_2 flux estimates by transport model inversions, Tellus, 55B, 522–529, 2003.

Mukai, H., Katsumoto, M., Ide, R., Machida, T., Fujinuma, Y., Nojiri, Y., Inagaki, M., Oda, N., and Watai, T.: Characterization of atmospheric CO_2 observed at two-background air monitoring stations (Hateruma and Ochi-shi) in Japan, in: Extended abstracts in the Sixth International Carbon Dioxide Conference, Sendai, Japan, Tohoku University, 108–111, 2001.

Nakazawa, T., Aoki, S., Fukabori, M., and Tanaka, M.: The concentration of atmospheric carbon dioxide on the summit of Mt. Fuji (3776 m), J. Meteorol. Soc. Jpn., 62, 688–695, 1984.

NOAA/ESRL.: The 6th WMO/IAEA Round Robin Comparison Experiment, available at: http://www.esrl.noaa.gov/gmd/ccgg/wmorr/wmorr_results.php?rr=rr6&param=co2&group=group5, last access: 16 November 2016.

Saeki, T., Maksyutov, S., Sasakawa, M., Machida, T., Arshinov, M., Tans, P. P., Conway, T. J., Saito, M., Valsala, V., Oda, T., Andres, R. J., and Belikov, D.: Carbon flux estimation for Siberia by inverse modeling constrained by aircraft and tower CO_2 measurements, J. Geophys. Res.-Atmos., 118, 1100–1122, 2013.

Sawa, Y.: Chapter 6 Continuous Observations of CO at the Summit of Mt. Fuji, A Study of Variations and Transport of Carbon Monoxide in the Free Troposphere over the Western Pacific, PhD Thesis to Tohoku University, 2005.

Sawa, Y., Matsueda, H., Taguchi, S., Igarashi, Y., and Tsutsumi, Y.: Episodic enhancements of CO_2 and CO at the summit of Mt. Fuji (3776 m), Japan, Proceeding of the Seventh International Carbon Dioxide Conference, Boulder US Sep., 25–30, 2005.

Tans, P. P. and Keeling, R.: NOAA/ESRL, Scrips Institution of Oceanography (www.scrippsco2.ucsd.edu/), available at: www.esrl.noaa.gov/gmd/ccgg/trends/, last access: 1 April 2016.

Tsutsumi, Y., Zaizen, Y., and Makino, Y.: Tropospheric ozone measurement at the top of Mt. Fuji, Geophys. Res. Lett., 21, 1727–1730, 1994.

Thoning, K. W., Tans, P. P., and Komhyr W. D.: Atmospheric carbon dioxide at Mauna Loa Observatory, 2. Analysis of the NOAA GMCC data, 1974–1985, J. Geophys. Res., 94, 8549–8565, 1989.

Tohjima, Y., Mukai, H., Hashimoto, S., and Patra, P. K.: Increasing synoptic scale variability in atmospheric CO_2 at Hateruma Island associated with increasing East-Asian emissions, Atmos. Chem. Phys., 10, 453–462, doi:10.5194/acp-10-453-2010, 2010.

Van der Werf, G. R., Dempewolf, J., Trigg, S. N., Randerson, J. T., Kasibhatla, P. S., Gigio, L., Murdiyarso, D., Peters, W., Morton, D. C., Collatz, G. J., Dolman, A. J., and DeFries, R. S.: Climate regulation of fire emissions and deforestation in equatorial Asia, P. Natl. Acad. Sci. USA, 105, 20350–20355, 2008.

Watanabe, F., Uchino, O., Joo, Y., Aono, M., Higashijima, K., Hirano, Y., Tsuboi, K., and Suda, K.: Interannual variation of growth rate of atmospheric carbon dioxide concentration observed at the JMA's three monitoring stations: Large increase in concentration of atmospheric carbon dioxide in 1998, J. Meteorol. Soc. Jpn., 78, 673–682, 2000.

WMO: World Data Center for Greenhouse Gases (WDCGG) Data Summary 39, Tokyo, 77–89, 2015.

Zeng, J. and Fujinuma, Y.: New web site launched for online air trajectory calculation, EOS, Transactions American Geophysical Union 85, 482 pp., 2004.

Zhang, H. F., Chen, B. Z., van der Laan-Luijikx, I. T., Chen, J., Xu, G., Yan, J. W., Zhou, L. X., Fukuyama, Y., Tans, P. P., and Peters, W.: Net terrestrial CO_2 exchange over China during 2001–2010 estimated with an ensemble data assimilation system for atmospheric CO_2 J. Geophys. Res.-Atoms., 199, 3500–3515, doi:10.1002/2013JD021297, 2014.